Analysis of the effect of characteristic parameters and operating conditions on exergy efficiency of alkaline water electrolyzer

Shunliang Ding[1], Bin Guo[1, 2, 3], Song Hu [2, *], Junjie Gu[3], Fuyuan Yang[3, **], Yangyang Li[3, ***], Jian Dang[3], Biao Liu[3], Jugang Ma[3]

1: School of Mechanical and Power Engineering, Zhengzhou University, 450001, Zhengzhou, China

2: School of Mechanical Engineering, University of Science and Technology Beijing, 100083, Beijing, China

3: State Key Laboratory of Automotive Safety and Energy, Tsinghua University, 100084, Beijing, China

Abstract: The technology of alkaline water electrolyzer (AWE) for hydrogen production provides a promising way to storage and utilize the renewable energy. Further improvement of AWE efficiency is one of the main research directions at present. In this paper a thermodynamics-electrochemical model of AWE is established, then this model is applied to detailly analyze the influences of characteristic parameters (electrode conductivity, distance between the electrode and diaphragm, diaphragm porosity and tortuosity, electrolyte concentration, bubble coverage) and operating conditions (temperature and pressure) on over-potential and exergy efficiency of AWE. Analysis results show that activation over-potential, compared with ohmic over-potential, presents more significant influence on the cell voltage and exergy loss. Ohmic over-potential changed most obviously with current density under the condition of 358K and 30wt% KOH concentration. Diaphragm resistance accounts for the largest proportion of total ohmic resistance exergy loss, followed by electrolyte and bubbles,

* Corresponding Author at School of Mechanical Engineering, University of Science and Technology Beijing, 100083, Beijing, China. *E-mail address:* husong_90@163.com (Song Hu)

** Corresponding Author at State Key Laboratory of Automotive Safety and Energy, Tsinghua University, 100084, Beijing, China. *E-mail address:* fyyang@tsinghua.edu.cn (Fuyuan Yang)

*** Corresponding Author at State Key Laboratory of Automotive Safety and Energy, Tsinghua University, 100084, Beijing, China. *E-mail address:* lyy025930@163.com (Yangyang Li)

and electrode resistance can be almost ignored. By quantifying and comparing the effect of each parameter on exergy efficiency, it is found that the diaphragm porosity has the most obvious effect on exergy efficiency among each characteristic parameter, the effect of electrode gap is the second in impact, the effect of bubble coverage is less important, but studies related to it are valuable and the effect of electrode conductivity can be largely ignored. The influence of temperature on exergy efficiency is more significant than that of pressure in operating conditions. This paper can provide reference for the selection of each parameter through conducted quantitative comparative analysis, which is of great significance for energy loss analysis and performance optimization of AWE device.

Key words: Alkaline water electrolysis; Exergy efficiency; Characteristic parameters; Operating conditions.

1. Introduction

Hydrogen is an important energy carrier for building a diversified energy supply system with clean energy, which is regarded as an essential link between renewable and traditional energy in the future smart energy system [1-3]. Hydrogen mainly comes from fossil energy (coal, natural gas, etc.) or reforming production of liquid hydrocarbons at this stage, which will cause environmental pollution and over-exploitation of fossil fuels [4-6]. As a new type of hydrogen production technology, water electrolysis to produce hydrogen from renewable energy has attracted more and more attention. At present, only about 4% of the global hydrogen is produced by

hydrolysis [7], mainly due to the limited infrastructure for hydrogen production by water electrolysis and the high economic cost of hydrogen production. Recent studies have shown that the cost of renewable hydrogen production needs to be reduced by half in order to be economically competitive with hydrogen produced from fossil fuels [8-10].

The most common water electrolysis technology includes alkaline water electrolysis (AWE), polymer exchange diaphragms water electrolysis (PEM), and solid oxides water electrolysis. AWE is the earliest developed and most mature technology among these three, which currently has the highest market share in the field of water electrolysis [11]. System modelling is one of the main areas of current research in AWE electrolyser and electrochemical modelling has received a lot of attention as the core of modelling work on water electrolysis systems. Ulleberg et al. [12] developed an empirical model for the accurate prediction of electrochemical properties, this model has been widely used by many authors as it requires a low number of experimental parameters to construct the polarization curve that characterizes the operation of electrolyzer, allowing to perform estimations for large scale applications such as the prediction of electrolysis voltage and hydrogen production rate [13-15]. Henao et al. [16] developed a more complete electrochemical mechanistic model and integrated it into an electrical simulation system for research. Olivier et al. [7] summarized the existing work and completed a very comprehensive review of electrochemical modeling for researchers. Jang et al. [17, 18] studied the effects of temperature and pressure on the performance of AWE systems on this basis and found that increasing

temperature facilitates a reduction in ohmic overpotential and that increasing the pressure at high current density leads to a reduction in activation and ohmic over-potential.

At present, the electrolytic efficiency of AWE is 59%-70%. Further improvements in electrolytic efficiency are also a major area of current research, but high ohmic and activation over-potential loss have become the main factors to limit its efficiency [19, 20]. In order to improve the electrolysis efficiency of AWE, many researchers have carried out various studies. Bakker et al. [21] studied the influence of pressure swings on cell voltage based on rectangular electrochemical flow cell experimental platform, and the results showed that pressure swings could reduce the influence of voltage accumulation caused by the shield layer formed by bubbles on electrode surface. Phillips et al. [22] researched the structure advantages of zero-gap alkaline electrolyzer compared with the traditional design. It was found that small electrode gap has compact design and high electrolytic efficiency, mainly because it could force bubbles to release from the back of the electrode which could reduce the ohmic resistance of electrolyte and bubbles between the two electrodes. Haverkort et al. [23] studied the voltage loss in the structure of zero-gap electrolyzer and found that, compared with the traditional zero-gap electrolyzer, the electrode gap of 0.2 mm could eliminate ohmic loss of most bubbles, thus improving the electrolytic efficiency. Li et al. [24] set up a simple experimental platform of electrolyzer and studied the influence of magnetic field on cell voltage and efficiency. The results showed that the optimal layout of electrode and magnetic field could induce bubbles to detach from the electrode surface, which was

beneficial to reduce cell voltage and improve electrolytic efficiency. Wang et al. [25] studied the relationship between cell voltage and gravity coefficient through establishing a cylindrical centrifugal electrolyzer experimental platform that could provide different gravity coefficients. The results showed that the electrolysis of water is obviously enhanced under the action of supergravity field, and the cell voltage decreases greatly under the higher gravity coefficient and current density, in which the ohmic voltage drop is the main influence. Li et al. [26] studied the influence of ultrasonic wave on electrolysis process based on the experimental platform of electrolyzer under the action of ultrasonic wave. It was found that the voltage is greatly reduced, hydrogen production efficiency is increased by 5-18% and energy saving is about 10-25% under ultrasonic field, especially under high current density and low electrolyte concentration. Even though there are many researches pay attention on how to improve the electrolytic efficiency of AWE, but most of them just focus on part of the structure or operating parameters, fail to reveal the influence rule of each parameter on energy efficiency and over-potential, moreover, the variation trend of parameter-energy efficiency/over-potential and its deeper mechanism in a wide range of steady-state conditions have not been fully displayed.

There exist many evaluation indexes of electrolytic efficiency, including energy efficiency, voltage efficiency, thermal efficiency and so on. Energy efficiency bases on the first law of thermodynamics, which reflects the proportion of total input energy converted to hydrogen chemical energy. However, the energy input to the electrolyzer is not only used in the electrolytic process, but also consumed in the form of useless

energy and heat transfer. Therefore, the analysis based on energy efficiency cannot provide accurate reference for the influence of various parameters on electrolytic efficiency, which may mislead the analysis results [27]. While, exergy efficiency is based on the principle of energy conservation, mass conservation and the second law of thermodynamics, reflecting the efficiency at which the maximum useful energy used for the electrolysis reaction converts to hydrogen chemical energy in a particular environment. It integrates the electrochemical characteristics into thermodynamic analysis to accurately analyze the rationality of energy utilization and the influence of various parameters on electrolysis efficiency. Meng Ni et al. [28, 29] studied the electrochemical-thermodynamic characteristics of the two hydrogen production methods of PEM and solid oxide steam electrolyzer respectively by means of exergy efficiency analysis method. However, those study were mainly focused on the influences of operating parameters such as temperature and current density on exergy efficiency, without detailed analysis of the influences of different design parameters. Khalid et al. [27] studied the influences of design parameters in AWE electrolyzer on exergy efficiency and energy consumption. However, due to many deviations in the modeling process and no verification with experimental data, the calculation results were inconsistent with the actual situation and could not provide reference for the optimization of electrolyzer parameters.

According to the above literature investigation, there is still no reliable and comprehensive study on the effects of AWE characteristic parameters and operating conditions on exergy efficiency. This work will establish an AWE electrochemical-

thermodynamic model and combine with exergy efficiency analysis method to carry out relatively comprehensive analysis of AWE characteristic parameters and operating conditions on exergy efficiency and voltage loss. In Section 2, the AWE electrochemical-thermodynamic model will be firstly established. Then, in Section 3, the exergy efficiency analysis method will be introduced. And in Section 4, the experimental setup and detailed parameter setting will be introduced. At last, in Section 5, the influences of characteristic parameters (electrode conductivity, electrode gap, diaphragm thickness, electrolyte concentration, bubble coverage) and operating conditions (pressure, temperature) on cell voltage and exergy efficiency will be analyzed. Through the comprehensive comparative analysis of the influence of each parameter, it can provide a theoretical guidance for how to optimize the electrolytic efficiency.

2. AWE physics model

Electrical energy is the main energy source in electrolysis and also an important part of exergy efficiency analysis in AWE electrolyzer. Electrochemical modeling reflects the composition of cell voltage and its relationship with current. Accurate electrochemical modeling is the precondition to analyze the influence of different parameters on exergy efficiency of AWE. This section will build a comprehensive electrochemical model including the reversible voltage, ohmic over-potential and activation over-potential. Diffusion over-potential is usually not considered, because the operating current density is low and the electrodes are always immersed in the

electrolyte in AWE electrolyzer.

2.1. AWE reaction principle of hydrogen production

AWE hydrogen reaction process contents both electron and ion transfer. After a direct current (DC) is supplied between the two electrodes, electrons flow from the negative pole of the DC power source to the cathode, where they are combined with hydrogen ions on the cathode to form hydrogen gas. To maintain charge balance, hydroxide ions are transferred through the electrolyte solution and crossover diaphragm to the anode, where they release electrons and generate oxygen. The released electrons are returned to the positive pole of the DC power supply. The chemical equation for this reaction is as follows:

$$\text{Cathode: } 2H_2O + 2e^- \rightarrow H_2\uparrow + 2OH^-, \quad E_{cat}^0 = -0.828\ \text{V} \tag{1}$$

$$\text{Anode: } 2OH^- \rightarrow H_2O + \frac{1}{2}O_2\uparrow + 2e^-, \quad E_{an}^0 = 0.404\ \text{V} \tag{2}$$

$$\text{Total response: } H_2O \rightarrow H_2\uparrow + \frac{1}{2}O_2\uparrow, \quad E_{rev}^0 = 1.23\ \text{V} \tag{3}$$

Where E_{cat}^0、E_{an}^0 respectively represents the voltages of the anode and cathode under standard conditions; E_{rev}^0 represents the reversible voltage under standard conditions.

2.2. Electrochemical modeling of AWE hydrogen production

The polarization curve (*I-V*) is an important index to evaluate the performance of electrolyzer, which is affected by the design and operation parameters. The total cell voltage of AWE is composed of reversible voltage V_{rev}, activation over-potential of cathode and anode V_{act}, ohmic over-potential V_{ohm} and concentration over-potential

V_{diff}. Due to the low current density and the electrode is always immersed in the electrolyte during the reaction process, concentration over-potential is usually not considered. The total cell voltage composition is shown in Eq. (4). V_{rev}, V_{act}, and V_{ohm} are modeled in sections 2.2.1, 2.2.2, and 2.2.3, respectively.

$$V_{\mathrm{cell}} = V_{\mathrm{rev}} + V_{act} + V_{\mathrm{ohm}} \tag{4}$$

2.2.1. Reversible voltage

Reversible voltage is the minimum cell voltage for water to meet electrolytic conditions, which is about 1.23 V under standard conditions. In the reaction process, the value of V_{rev} will be affected by operating temperature and pressure, which can be calculated as follows [30]:

$$V_{\mathrm{rev}} = V_{rev}^{0} + \frac{RT}{2F}\ln\left[\frac{(P-P_{H2O})^{1.5}}{\alpha_{H2O}}\right] \tag{5}$$

Where R is the gas constant ($R = 8.314\ \mathrm{J/(mol \cdot K)}$); T is the operating temperature in electrolyzer; F is the Faraday constant (F=96485); P is the operating pressure in electrolyzer; P_{H2O} represents the partial pressure of water vapor in electrolyzer; α_{H2O} represents the activity of water. P_{H2O} can be estimated by empirical formula related to T and the molar concentration of electrolyte m [31]:

$$\begin{aligned}\log P_{H_2O} = {} & -0.01508m - 0.0016788m^2 + 2.25887\times10^{-5}m^3 \\ & + (1 - 0.0012062m + 5.6024\times10^{-4}m^2 - 7.8228\times10^{-6}m^3) \\ & \times \left(35.4462 - \frac{3343.93}{T} - 10.9\log T + 0.004165T\right)\end{aligned} \tag{6}$$

α_{H2O} in KOH solution within the range of 273 K-423 K can be estimated by the following formula [31]:

$$\log \alpha_{H_2O}(\mathrm{KOH}) = -0.02255m + 0.001434m^2 + (1.38m - 0.9254m^2) \tag{7}$$

)

2.2.2. Activation over-potential

The transfer of electron from the reactants to the electrodes must overcome the energy step which is called the activation energy. Activation over-potential is related to the activation energy of the electrochemical reaction on the electrode, which is namely the voltage consumed in the duration when the reaction breaks the equilibrium state and starts to proceed forward, which is closely related to the electrocatalytic activity of the electrode material [32]. In the process of reaction, the bubbles attach to the electrode surface will also have an influence on V_{act}. Considering the influence of bubbles, V_{act} can be expressed as follows [7]:

$$V_{act} = \frac{RT}{\mathrm{n}\alpha_a F}\ln\left(\frac{J}{J_{0,a}(1-\theta)}\right) + \frac{RT}{\mathrm{n}\alpha_c F}\ln\left(\frac{J}{J_{0,c}(1-\theta)}\right) \quad (8)$$

Where n represents the amount of charge transferred when producing 1 mol hydrogen ($\mathrm{n} = 2$); α_a and α_{c} respectively denote the charge transfer coefficients of the anode and cathode, which can be calculated by empirical temperature-dependent formulas, as shown in Eq. (9) and Eq. (10) [30]; J is current density; $J_{0,a}$、$J_{0,\mathrm{c}}$ respectively represent the exchange current density of anode and cathode which is shown in Eq. (11) and Eq. (12) when nickel material is used as electrode [17], where T_0、P_0 respectively represent the initial reference temperature and pressure; θ is the bubble coverage on the electrode surface, Its empirical formula is shown in (13) [17]:

$$\alpha_a = 0.0675 + 0.00095T \quad (9)$$

$$\alpha_{\mathrm{c}} = 0.1175 + 0.00095T \quad (10)$$

$$J_{0,a} = 0.9\left(\frac{P}{P_0}\right)^{0.1} \exp\left[-\frac{42000}{RT}\left(1-\frac{T}{T_0}\right)\right] \tag{11}$$

$$J_{0,c} = 1.5\left(\frac{P}{P_0}\right)^{0.1} \exp\left[-\frac{23000}{RT}\left(1-\frac{T}{T_0}\right)\right] \tag{12}$$

$$\theta = 0.023(J)^{0.3}\left(\frac{T\ P_0}{T_0\ P}\right)^{\frac{2}{3}} \tag{13}$$

2.2.3. Ohmic over-potential

AWE electrolyzer is usually composed of several electrolyzer cells connected in series. The electrons and ions migration paths in zero-gaps electrolyzer are shown in Fig. 1(a). After closing current circle, the electrons will be transferred to the cathode through the polar frame and the reduction reaction will take place at the surface of the electrode. Then, the generated hydroxide ions will pass through the electrolyte and crossover diaphragm to the anode, where an oxidation reaction will take place and the lost electrons will continue to pass through the polar frame to the next electrolyzer cell. The composition of ohmic resistance in AWE electrolyzer can be obtained based on the migration paths of electrons and ions, which is included anode resistance R_a、cathode resistance R_c、electrolyte resistance R_{ele}, bubble resistance R_{bubble}, diaphragm resistance R_{mem}, external line resistance R_1, etc. Because the ohmic over-potential caused by external line resistance is small, therefore it is usually ignored in modeling analysis. So that, the total ohmic over-potential can be expressed as follows:

$$V_{\mathrm{ohm}} = (R_c + R_a + R_{ele} + R_{mem} + R_{\mathrm{bubble}}) \times I \tag{14}$$

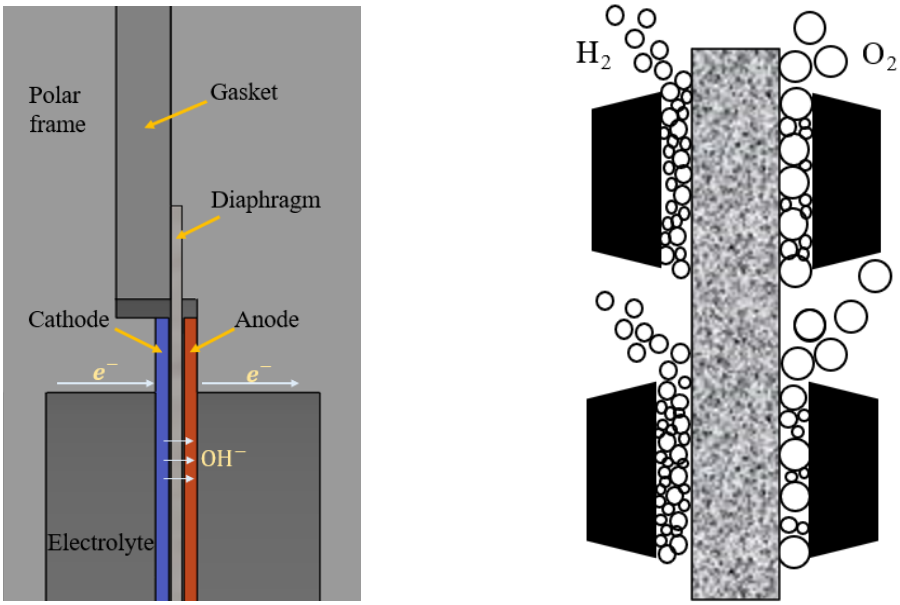

(a) (b)

Fig. 1. Zero-gap AWE electrolyzer. (a) Electron and ion migration paths in electrolyzer. (b) Distribution of bubbles producing sites on electrode surface.

The resistance of the electrode is mainly related to the electrode structure and material properties, the anode resistance R_a and cathode resistance R_c can be expressed as follows:

$$R_a = \frac{1}{\sigma_a}\left(\frac{\delta_a}{S_a}\right) \tag{15}$$

$$R_c = \frac{1}{\sigma_c}\left(\frac{\delta_c}{S_c}\right) \tag{16}$$

Where δ_a、δ_c indicate the thickness of cathode and anode; S_a、S_c indicate the area of anode and cathode; σ_a、σ_c represent the conductivity of the anode and cathode, which is related to the material properties of the electrode itself. Currently, porous nickel is mostly used as the electrode material of AWE electrolyzer, and its conductivity can be estimated as a function related to T [17]:

$$\sigma_a = \sigma_c = \sigma_{Ni} = 60000000 - 279650T + 532T^2 - 0.38057T^3 \tag{17}$$

From the perspective of ion migration path, the resistance of electrolyte represents the resistance of ion migration from the cathode surface to the diaphragm and then from the other side of the diaphragm to the anode. While, the electrolyte resistance outside of the two electrodes is usually ignored. So that, R_{ele} can be estimated by the current mainstream modeling method [16, 17]:

$$R_{ele} = \frac{1}{\sigma_{\mathrm{ele}}}\left(\frac{d_{am}}{s_a} + \frac{d_{cm}}{s_c}\right) \tag{18}$$

Where, σ_{ele} represents the conductivity of the electrolyte; d_{am} and d_{cm}indicate the distances from the anode and cathode to the diaphragm respectively. For the traditional non-zero-gap electrolyzer, the values of d_{am} and d_{cm} can be taken as the actual physical distance between the electrode and the diaphragm. However, for the zero-gap structure, the electrode and the diaphragm are in direct contact, what's more, V. Kienzlen et al. [33] found that bubbles were mainly generated on the opposite side of the diaphragm, as shown in Fig. 1(b), this indicates that the reaction sites on the electrode surface are mainly distributed on the contact surface between electrode and diaphragm. It means that the value of the distance between electrode and diaphragm in zero-gap electrolyzer should be 0, but this will lead to the resistances of electrolyte and bubble part are 0, which obviously does not conform to the actual situation. In this work, d_{am} and d_{cm} are both taken as 1.2 mm by fitting the modeling results and the experimental data, the detail fitting process will be shown in Section 5.1. In Section 5.2.1, the correlation between electrode gap and exergy efficiency will be studied detailly.

For the ionic conductivity of KOH solution, this work adopts the following

empirical formula given by Gilliam et al. [34] to estimate its value:

$$\sigma_{KOH} = -2.041m - 0.0028m^2 + 0.005332mT + 207.2\frac{m}{T} + 0.0 - 0.0000003m^2T^2 \quad (19)$$

Because diaphragm materials are not conductive, therefore ions are mainly transmitted through diaphragm pores filled with KOH solution. Therefore, diaphragm resistance R_{mem} is mainly related to its own structural characteristics and the conductivity of KOH solution [35]:

$$R_{mem} = \frac{\delta_m \cdot \tau_m}{p_m \cdot \sigma_{KOH} \cdot S_m} \quad (20)$$

Where δ_m is diaphragm thickness; p_m is diaphragm porosity; $\tau_m$indicates the diaphragm tortuosity; S_m is the diaphragm cross-sectional area.

During the reaction, bubbles on the surface of the electrode continue to accumulate and grow. Once the buoyancy and shear force exceed the adhesion force of the electrode surface, the bubbles will be separated from the electrode surface. The bubbles separation from the electrode surface is affected by the roughness of the electrode, the contact angle and the velocity of the electrolyte near the electrode surface. The bubbles will hinder the reactive ion transport in the electrolyte and increase the length of ion transmission path, thus increase the resistance of the whole. The ion transmission route when with and without bubbles effect as shown in Fig. 2. Bubble resistance usually refers to the increased electrolyte resistance after bubbles entering the solution from the electrode surface, bubbles on the surface of the electrode mainly affect activation over-potential. The resistance of the bubble part $R_{b\mathrm{ubble}}$ can be estimated as [16]:

$$R_{bubble} = R_{ele} \cdot \left[\frac{1}{(1-\frac{2}{3}\theta)^{\frac{3}{2}}} - 1 \right] \tag{21}$$

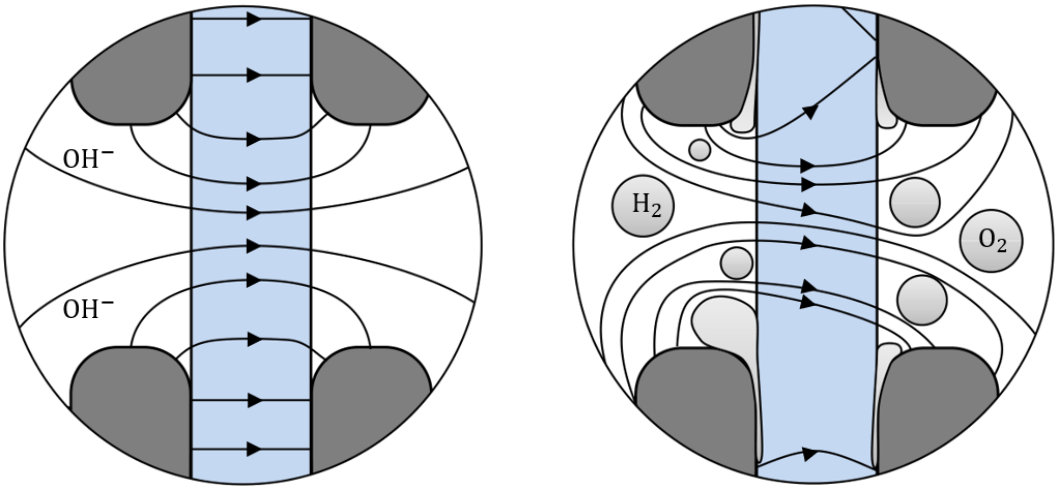

Fig. 2. Influence of bubbles on ions transport. (a)ion transport without bubbles and (b) ion transport path with bubbles [23].

3. Exergy efficiency analysis method

This section will compare the analysis methods of energy efficiency and exergy efficiency and point out the advantages of exergy efficiency analysis. First of all, it is necessary to calculate the theoretical energy required for water electrolysis, its total energy demand is expressed as follows:

$$\Delta H = \Delta G + Q = \Delta G + T\Delta S \tag{22}$$

Where ΔH stands for enthalpy change which reflects the energy demand of water decomposition under certain conditions (285 KJ/mol under standard conditions); ΔG is Gibbs free energy; Q is the heat absorbed during the reaction. It can be seen from Eq. (22) that the electrolysis process requires the joint action of electric energy and heat

energy. In the actual electrolysis reaction process, over-potential due to ohmic and activation resistances, heat exchange between the electrolyzer and environment and energy losses due to gas output are unavoidable [36]. Therefore, the electrolysis efficiency can reflect the utilization degree of energy, the quality of system performance and the influence of each parameter on performance.

From the perspective of energy efficiency, it represents the efficiency of converting energy input to hydrogen chemical energy, as shown below [29]:

$$\eta_{\mathrm{en}} = \frac{LHV_{H_2} \cdot \dot{n}_{H_2}}{Q_{electric} + Q_{heat,H_2O} + Q_{heat,cell}} \tag{23}$$

Where LHV_{H_2} represents the low calorific value of 1mol hydrogen; $\dot{n}_{H_2}$ denotes the rate of hydrogen production, which can be expressed as a function of current I and the number of electrolytic chambers n_c [12]:

$$\dot{n}_{H_2} = \frac{\mathrm{n}_c \cdot I}{2F} \tag{24}$$

$Q_{electric}$ indicates the power input rate:

$$Q_{electric} = I \cdot V_{\mathrm{cell}} \tag{25}$$

Q_{heat,H_2O} represents the heat energy input rate with water after heating. Assuming that the input rate of water is equal to the consumption rate of water in the electrolyzer, and that the temperature of water input after heating is the same as that in the electrolyzer, so the heat energy input rate with water can be expressed as [37]:

$$Q_{heat,H_2O} = Q_{heat,H_2O}^{max} \cdot \varepsilon = \dot{n}_{H_2O} \cdot (H_{H_2O}^{T} - H_{H_2O}^{T_0}) \cdot \varepsilon \tag{26}$$

Where Q_{heat,H_2O}^{max} represents the theoretical maximum heat exchange rate between the two liquids; ε represents the effective heat exchange coefficient between two different

liquids; $\dot{n}_{H_2O}$ refers to the rate of water consumption during the reaction which is equal to the $\dot{n}_{H_2}$; $H_{H_2O}^{T}$ and $H_{H_2O}^{T_0}$represent the enthalpy of water at temperature T and initial reference temperature T_0, respectively.

$Q_{heat,cell}$ represents the heat input rate. The reaction is exothermic process when the voltage is greater than the thermoneutral cell voltage (standard condition of 1.48 V), at this case the additional heat input is no longer needed [28]. The heat energy input rate of the electrolytic cell is expressed as follow when cell voltage less than thermoneutral cell voltage.

$$Q_{heat,cell} = \mathrm{T}\Delta\mathrm{S} - (V_{\mathrm{cell}} - V_{rev}) \cdot I \tag{27}$$

For energy efficiency analysis method, the value of energy input stands for the total energy input. The energy efficiency cannot correctly reflect the actual energy conversion efficiency in electrolytic reaction. In view of this defect for energy efficiency, this paper adopts the exergy efficiency analysis method, which is more reasonable than energy efficiency when analyzing the influence of various parameters on the electrolysis efficiency. Exergy efficiency represents the proportion of the maximum useful energy actually converted to hydrogen chemical energy during electrolysis reaction, its calculation is as shown below [29]:

$$\eta_{\mathrm{exergy}} = \frac{E_{H_2} \cdot \dot{n}_{H_2}}{Q_{electric} + E_{heat,H_2O} + E_{heat,cell}} \tag{28}$$

Where, E_{H_2} represents the standard chemical exergy contained in 1mol hydrogen at 298 K and 1 bar with the value of 236.09 $\mathrm{KJ/mol}$ [38], which is a characteristic of hydrogen. E_{heat,H_2O} represents the exergy input rate with water at a certain

temperature, which can be expressed by Q_{heat,H_2O} and the heat source temperature T_S [28]:

$$E_{heat,H_2O} = Q_{heat,H_2O} \cdot \left(1-\frac{T_0}{T_S}\right) \quad (29)$$

$E_{heat,cell}$ represents the exergy input rate of external heat, which can be expressed as a function of $Q_{heat,cell}$, as shown below [28]:

$$E_{heat,cell} = Q_{heat,cell} \cdot \left(1-\frac{T_0}{T}\right) \quad (30)$$

4. Experimental setup and parameter setting

An AWE electrolyzer experimental bench at the State Key Laboratory of Automotive Safety and Energy in Tsinghua University is applied to obtain the experimental data, and its main structural components are shown in Fig. 3. This electrolyzer is with a zero-gap electrode structure, nickel electrode and a 0.7 mm thick PPS fabric diaphragm. The experimental data for the calibration of the *I-V* curve was carried out at 1.6 MPa and 358 K. More detailed parameters in the experimental bench and model are shown in Table 1.

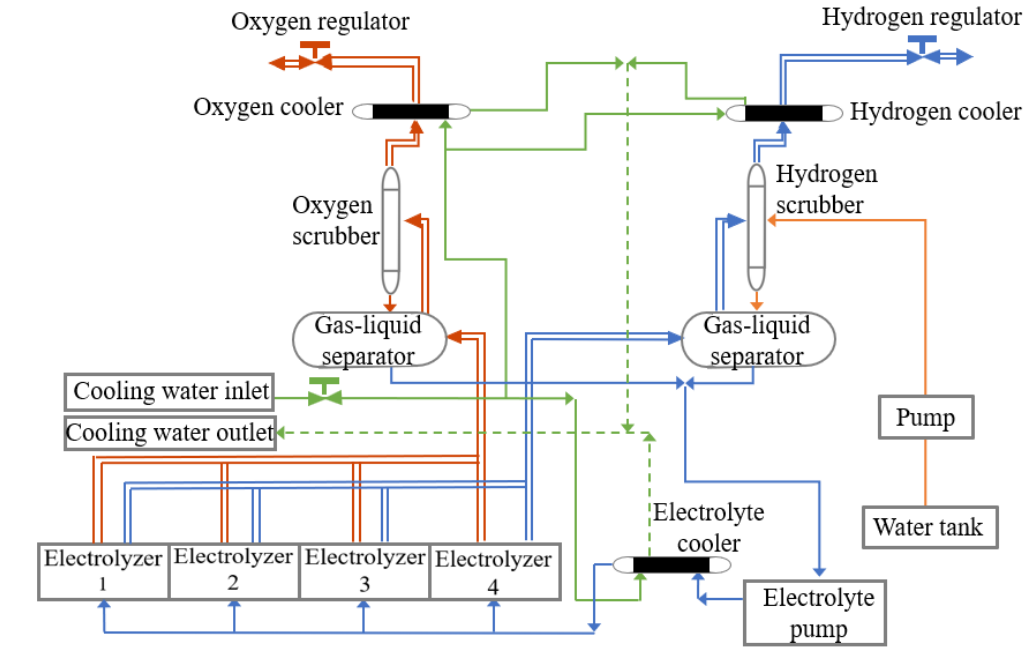

(a)

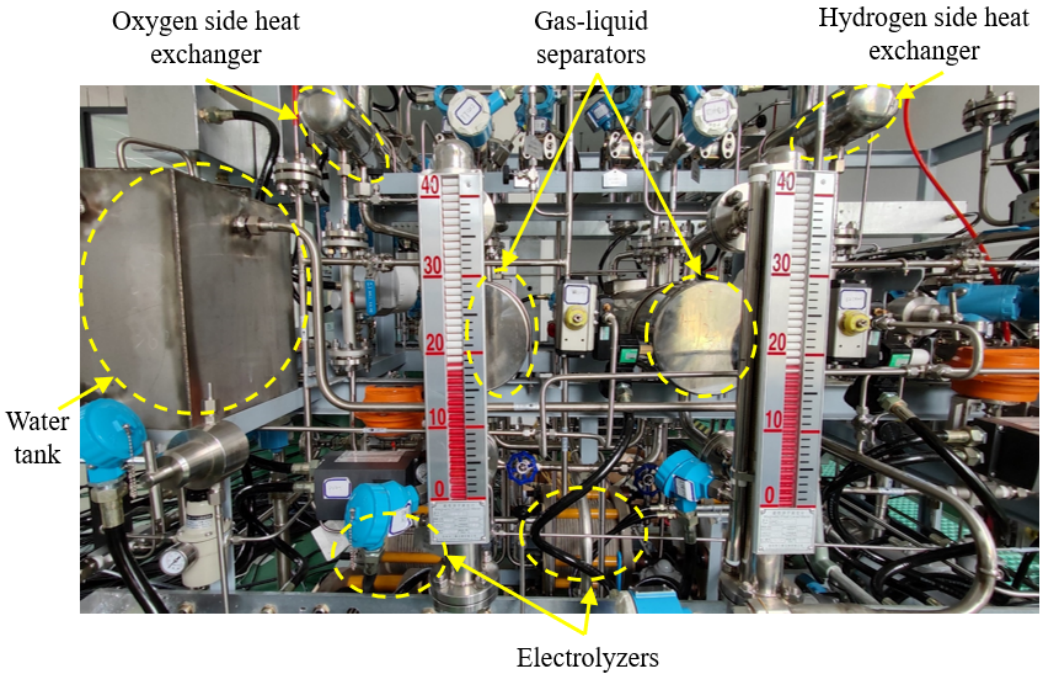

(b)

Fig. 3. AWE electrolyzer experimental bench at the State Key Laboratory of Automotive Safety and Energy in Tsinghua University. (a) System sketch and (b) main system components.

Table 1. Parameters used in AWE exergy efficiency analysis model.

Parameter	Value	Data source
n_c	8	Number of electrolytic cells
δ_a 、 δ_c(mm)	2	Provided by the manufacturer
δ_m(mm)	0.7	Provided by the manufacturer
d_{am} 、 d_{cm}(mm)	1.2	Distance between electrode and diaphragm
τ_m	5.2	[39]
p_m	0.65	[39]
LHV_{H_2}(KJ/mol)	282	Physical parameters
E_{H_2}(KJ/mol)	236.09	[27]
T(K)	358	Operating temperature of electrolyzer
T_0(K)	343	[17]
T_S(K)	373	Heat source temperature
P(Pa)	1.6×10^6	Pressure of electrolyzer
P_0(Pa)	1×10^6	Initial reference pressure
$H_{H_2O}^{T}$(KJ/mol)	6.038	Physical parameters
$H_{H_2O}^{T_0}$(KJ/mol)	1.521	Physical parameters
ε	0.8	[28]

5. Results and discussion

5.1. Analysis of cell voltage and exergy efficiency

In this section, a detailed analysis of the electrolytic voltage composition,

percentage and variation trend will be carried out based on experimental data, on this basis, the relationship between the exergy efficiency change under different operating conditions and the energy loss due to activation overpotential and ohmic overpotential for each part will be obtained.

V_{cell} and the proportion of V_{rev}、V_{act}、V_{ohm} in the total voltage when changing with current density are obtained based on the AWE comprehensive model established in Section 2.2. The simulation results are shown in Fig. 4(a), it can be seen that the simulation results are in good match with the experimental data. According to Fig. 4(a), V_{rev}, V_{act}, V_{ohm} all increase with the increase of current density, while V_{act} and V_{ohm} are the main reasons for the increase of cell voltage with the increase of current density. For V_{rev}, it only increases slightly while the growth rate of V_{act} decreases rapidly when current density increasing; under the condition of low current density (< 1000 A/m^2), V_{act} grows as a log function and plays a major role for the increasing of cell voltage; while under the condition of medium and high current density (> 1000 A/m^2), its growth rate becomes very slow. For V_{ohm}, its growth rate, when the current density is < 1000 A/m^2, is relatively slow but gradually accelerates and then, when the current density is >1000 A/m^2, keeps approximately constant with the increase of current density, and gradually becomes the major role for the increasing of cell voltage.

According to Fig. 4(a) and Fig. 4(b) from the longitudinal point of view, the proportion of over-potential in cell voltage increases with the increase of current density. At 1000 A/m^2 current density, the over-potential is 0.50 V which takes 30% of the total cell voltage, in which V_{act} and V_{ohm} are 0.45 V and 0.06 V with the proportions of 26.7% and 3.3%, respectively. The over-potential is mainly caused by V_{act}. At 5000 A/m^2 current density, the over-potential is 0.87 V which accounts for 42.1% of the total cell voltage. For this case, V_{act} and V_{ohm} are 0.58 V and 0.29 V with the

proportions of 28% and 14.1%, respectively. The over-potential is still mainly caused by V_{act}, even though V_{ohm} is greatly increased from 0.06 V to 0.33 V. As the current density increasing to 10000 $\mathrm{A/m^2}$, the over-potential increases to 1.22 V, accounting for 50.7% of the total cell voltage, among which V_{act} and V_{ohm} are 0.63 V and 0.59 V with the proportions of 26.1% and 24.6%, respectively. Compared with the case of 5000 $\mathrm{A/m^2}$, V_{act} increases slightly from 0.58 V (with a proportion of 28%) to 0.63 V (with a proportion of 26.1%), and V_{ohm} increases obviously from 0.29 V (with a proportion of 14.1%) to 0.59 V (with a proportion of 24.6%) due to the large increase of ohmic over-potential.

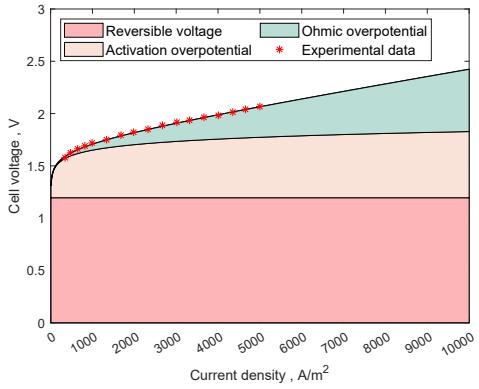

(a)

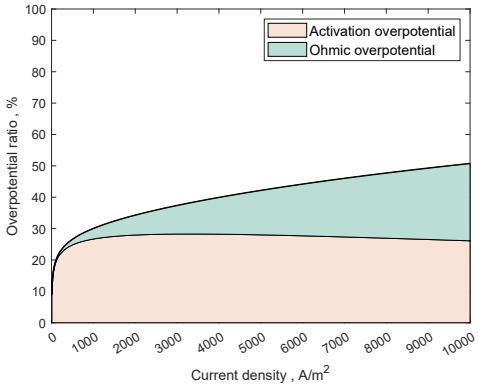

(b)

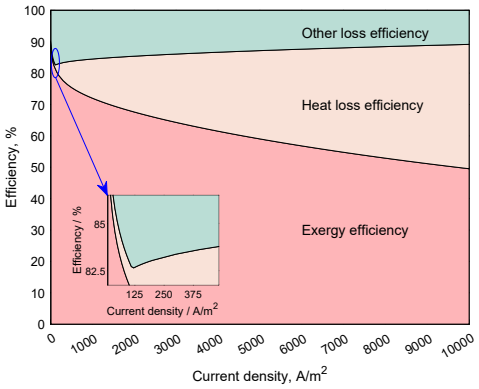

(c)

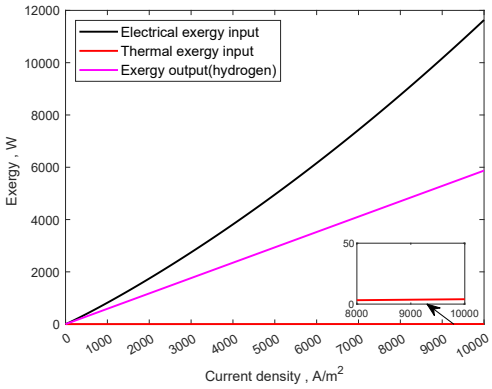

(d)

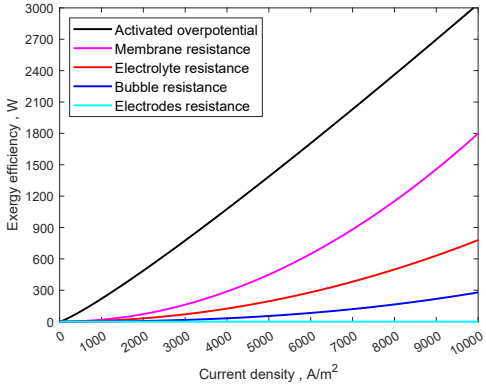

(e)

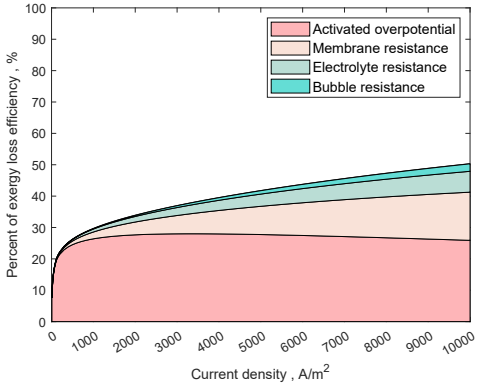

(f)

Fig. 4. Analysis of cell voltage and exergy efficiency. (a) Composition and variation trend of cell voltage. (b) The proportion of ohmic and activated over-potential in total cell voltage. (c) Exergy efficiency varies with current density. (d) Exergy input and output varied with current density. (e) Exergy loss caused by over-potential. (f) The proportion of exergy loss.

On the basis of the above analysis to obtain each voltage proportion and trend, the variation of efficiency with current density at 358 K is obtained as shown in Fig. 4(c). It can be seen that the exergy efficiency of the system decreases significantly from 82.2% to 59.2% by 23% when the current density increases from 100 A/m^2 to 5000 A/m^2. At low current density (< 1000 A/m^2), exergy efficiency decreases greatly, mainly caused by the rapid increase of activation over-potential. The exergy efficiency further decreases 8.7% from 59.2% to 50.5% which is significantly smaller compared with small current density when the current density continues to increase to 10000 A/m^2. It can also see from Fig. 4(c) that the change of exergy efficiency loss caused by thermal energy loss as a function of current density, which is called heat loss efficiency for short. The heat energy loss refers to the excess heat energy in addition to the heat energy

absorbed by electrolytic process, including the residual part of the input heat energy and the heat energy released by electrolytic reaction. The increase of heat loss efficiency is relatively slow and the value is very small (< 1.2%) when the current density is lower than 120 A/m^2, because the cell voltage and the reaction rate at this case is low which result the reaction is endothermic or slightly exothermic process. The heat loss efficiency significantly increases 26.8% from 1.2% to 28.0% when the current density increases from 120 A/m^2 to 5000 A/m^2, its proportion reaches to 38.5% when the current density increases to 10000 A/m^2 which is the main aspect of overall exergy loss efficiency.

The electrical exergy input, thermal exergy input and hydrogen exergy output changing with current density are shown in Fig. 4(d). The incoming electrical energy is 3 orders of magnitude higher than the incoming of heat exergy. Because the reaction is exothermic in most states, only a small amount of heat exergy can be input through electrolyte. Therefore, exergy efficiency is almost entirely determined by electric energy input. It can also see from Fig. 4(d) that the exergy difference between the input electrical exergy and the output hydrogen exergy continually growing which leaded by the increase of over-potential with the increase of current density.

Through the analysis results from Fig. 4(d), assuming that all the heat needed in the electrolysis process is provided by external heat and all the heat generated by over-potential is lost in the form of useless energy, exergy loss caused by ohmic and activated over-potential can be obtained, as shown in Fig. 4(e). The exergy loss caused by activated over-potential increases linearly with the current density and always

dominates the overall exergy loss when the current density increasing from 0 to 10000 A/m^2. Exergy loss caused by diaphragm, electrolyte and bubbles exponentially increases with current density, at the same time the percent of exergy loss accordingly increases. Exergy loss caused by the electrode is always the smallest part of overall exergy loss and increases slightly with current density. According to Fig. 4(f), the proportion of exergy loss from activated over-potential firstly rapidly increases and then slightly decreases with current density, mainly because exergy loss caused by ohmic over-potential (including diaphragm, electrolysis and bubble resistance over-potential) increases gradually from a small value. The exergy loss from activated over-potential reaches the maximum of 28.0% when the current density is 3400 A/m^2. The exergy loss slightly decreases 1.9% from 27.8% to 25.9% when current density increasing from 5000 A/m^2 to 10000 A/m^2. For the exergy loss from ohmic over-potential including diaphragm, electrolyte and bubble resistance, the part from diaphragm accounts for the largest proportion, followed by those from electrolyte and bubbles, moreover the part from electrode is very small and even can be ignored. The exergy loss from diaphragm increases 6.4% from 9.0% to 15.4% when current density increasing from 5000 A/m^2 to 10000 A/m^2, at the same time, the part from electrolyte slightly increases 2.7% from 3.9% to 6.6% and the part from bubbles slightly increases 1.4% from 1.0% to 2.4%. According to the above analysis, exergy loss caused by over-potential is quite large, so the development of AWE electrolyzer should mainly focus on reducing activation over-potential and researching parameters that have a greater influence on ohmic overpotential, such as electrode gap, diaphragm materials and structure.

5.2. Effects of characteristic parameters on exergy efficiency

According to the above analysis, over-potential is the main reason for the increase of cell voltage, energy consumption and exergy efficiency. This section will specifically discuss the parameters affecting the over-potential and provide theoretical guidance for optimizing electrolytic efficiency and reducing energy consumption. These parameters include electrode conductivity, electrode gap, diaphragm porosity, diaphragm tortuosity, electrolyte concentration and bubble coverage.

5.2.1. Influence of electrode parameters

Electrode conductivity is the main factor affecting electrode resistance. Fig. 5(a) analyzes the influence of electrode conductivity on electrode resistance and exergy efficiency at 358 K with 5000 $\mathrm{A/m^2}$ current density. When the electrode conductivity changes from $1000\ \mathrm{S/m}$ to 6000 $\mathrm{S/m}$, the electrode resistance decreases from $6.7 \times 10^{-5}\ \Omega$ to $1.1 \times 10^{-5}\ \Omega$, exergy efficiency only increases from 58.7% to 59.1% by a slight increase of 0.4%. The analysis results show that increasing electrode conductivity could reduce electrode resistance, thus reducing ohmic over-potential and improving exergy efficiency. However, because electrode resistance is small at first, so its proportion in the total resistance can be almost ignored. Therefore, improving electrode conductivity only presents a slight improvement effect on exergy efficiency.

The electrode parameter of electrode gap can affect electrolyte and bubble resistance by increasing the length of ion migration path. As shown in Fig. 5(b), electrolyte resistance increases from $0\ \Omega$ to $1.1 \times 10^{-3}\ \Omega$ and bubble resistance only increases from $0\ \Omega$ to $3.1 \times 10^{-4}\ \Omega$ when electrode gap changes from 0 mm

to 10 mm at 358 K with 5000 A/m^2 current density, so that, exergy efficiency significantly drops from 62.4% to 51.1% by 11.3%. Comparing with electrode conductivity, electrode gap has a much greater influence on exergy efficiency. Although the absolute zero-gap structure can ensure the minimum electrode gap, it may also increase the resistance of bubbles escaping from the electrode surface [23, 40]. Therefore, it is very important to determine the optimal electrode gap.

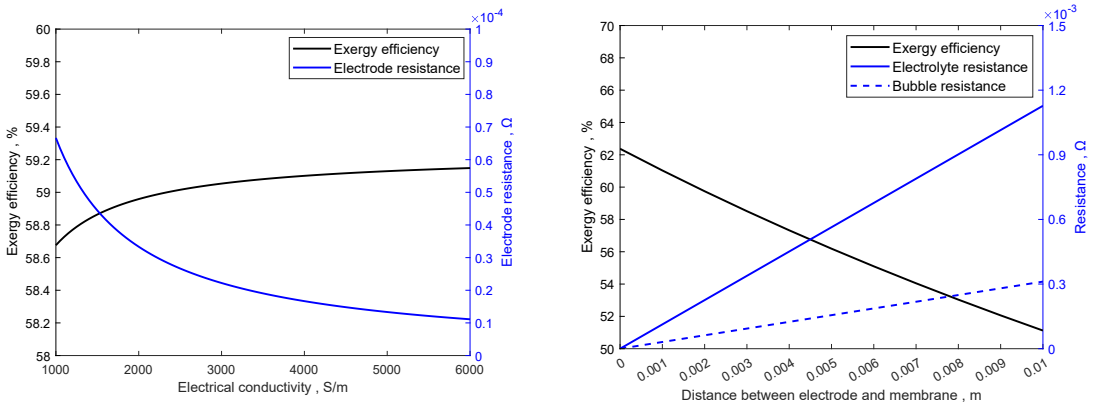

(a) **(b)**

Fig. 5. Effect of electrode parameters. (a) Influence of electrode conductivity on bubble resistance and exergy efficiency. (b) Influence of electrode gap on electrolyte and bubble resistance and exergy efficiency.

5.2.2. Influence of diaphragm and electrolyte parameters

AWE diaphragm is mainly used to separate cathode and anode to prevent cross-mixing of gases and allow OH^- through to ensure smooth reaction. There are many types of diaphragms, including asbestos diaphragm, PPS diaphragm, polysulfone diaphragm and so on. Porosity and tortuosity are two main parameters to affect the performance of diaphragm. The influences of porosity and tortuosity on the diaphragm resistance and exergy efficiency are shown in Fig. 6(a) and Fig. 6(a) respectively. As

can be seen from Fig. 6(a), the resistance of the diaphragm decreases from 3.7×10^{-3} Ω to 6.2×10^{-4} Ω when the porosity increases from 0.1 to 0.6, and exergy efficiency increases significantly from 40.8% to 59.2% by 18.4%. Therefore, increasing the porosity is greatly beneficial to reducing the diaphragm resistance, thus improving exergy efficiency. However, increasing the porosity of the diaphragm is not the same as increasing the pore size of the diaphragm which will increase the amount of gas cross-mixing and then lead to the reduction of the electrolyzer operating range. As shown in Fig. 6(b), the diaphragm tortuosity is approximately linearly related to the diaphragm resistance with a negative correlation and exergy efficiency with a positive correlation. Increasing tortuosity will lead to the increase of the path length for ions to cross the diaphragm and then result in the diaphragm resistance increase. Tortuosity increasing from 1 to 6 causes the diaphragm resistance increasing from 1.3×10^{-4} Ω to 7.9×10^{-4} Ω, which leads to an exergy efficiency drops from 63.8% to 57.9% by 5.9%. Comparing with tortuosity, porosity presents a more significant effect on exergy efficiency.

Electrolyte concentration and temperature will affect the ionic conductivity, which will then affect the resistance of electrolyte, diaphragm and bubbles. It can be seen from Fig. 6(c) that the conductivity increases with the increase of temperature and molar concentration, but too high concentration cannot completely ionize the electrolyte, which will increase ion migration resistance and lead to the decrease of conductivity [34]. There is an optimal molar concentration correlated to maximize ionic conductivity for each different temperature, and its value will gradually increase with the

temperature. The optimal molar concentration is about 5 mol/L at 293 K, while it will increase about 2.8 mol/L to 7.8 mol/L when temperature increasing to 373 K. The influence of KOH conductivity on electrolyte, diaphragm, bubble resistance and exergy efficiency at 358 K with 5000 $\mathrm{A/m^2}$ current density is shown in Fig. 6(d). It can be seen that, when KOH molar concentration increasing from 1 mol/L to 7 mol/L, the resistance of diaphragm, electrolyte and bubbles will all decrease, in detail, diaphragm resistance is from 2.3×10^{-3} Ω to 6.2×10^{-4} Ω, electrolyte is from 9.7×10^{-4} Ω to 2.7×10^{-4} Ω, and bubble resistance is from 2.7×10^{-4} Ω to 7.5×10^{-5} Ω, at last, this will lead to a 15.9% increase from 43.4% to 59.3% in exergy efficiency. It can be obviously obtained that, compared with electrolyte and bubble resistance, diaphragm resistance presents the greatest sensitivity to electrolyte concentration, and the second is electrolyte resistance. Since the bubble resistance just accounts for a small proportion of the total electrical resistance, electrolyte concentration only has a small influence on it. The exergy efficiency rapidly increases from 0% to 52.1% when KOH molar concentration changing from 0 mol/L to 2 mol/L; it slowly increases 7.2% from 52.1% to 59.3% as the concentration increasing from 2 mol/L to 7 mol/L; while, it will remain constant or even slightly decrease when the concentration further increasing from 7 mol/L. This is mainly because improving electrolyte ionic conductivity can decrease over-potential and enhance electrochemical reaction. According to the above analysis, it can be seen that the ionic conductivity of electrolyte has a great influence with a wide range on resistance, therefore, the best electrolyte molar concentration should be selected according to the actual electrolyzer parameter settings to reduce the resistance

of electrolyte, diaphragm and bubbles to the greatest extent.

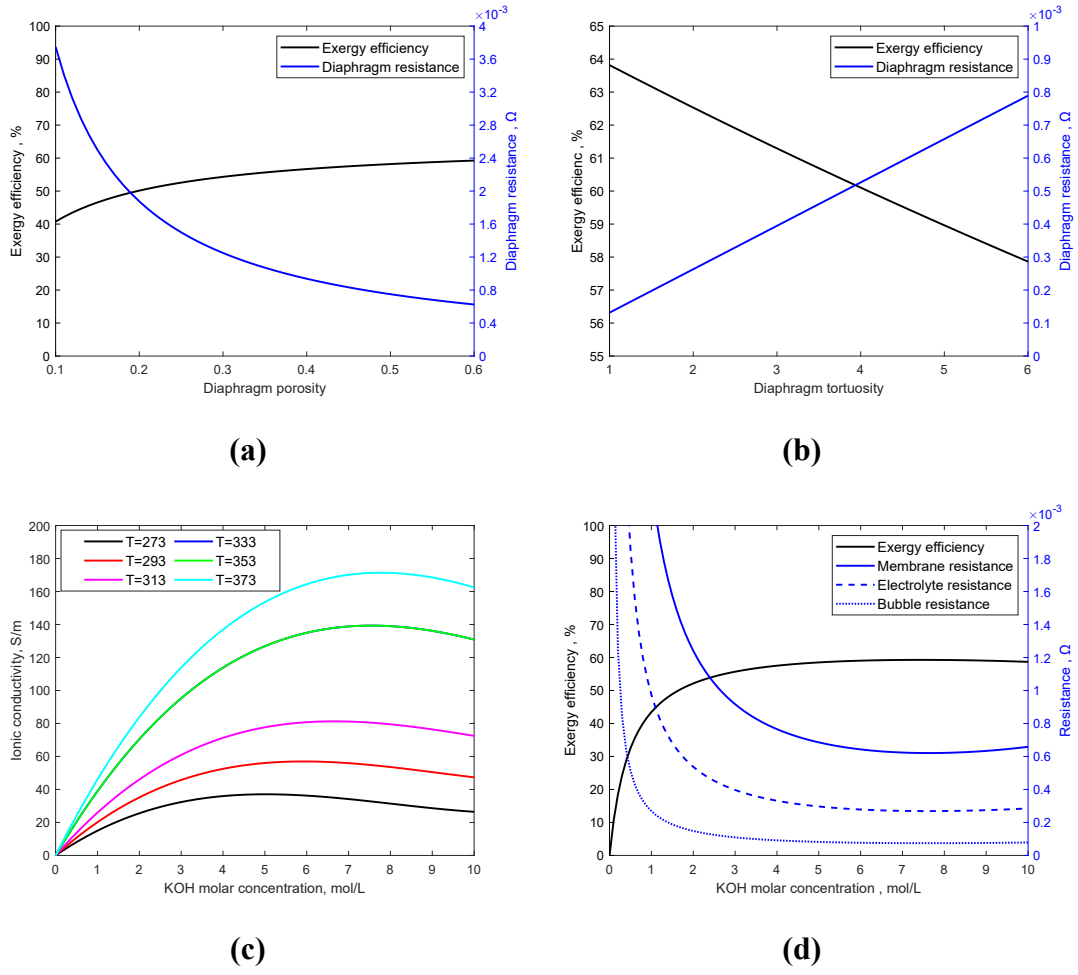

Fig. 6. Effect of diaphragm and electrolyte parameters. (a) Influence of diaphragm porosity on diaphragm resistance and exergy efficiency. (b) Influence of diaphragm tortuosity on diaphragm resistance and exergy efficiency tortuosity. (c) Influence of temperature and concentration on conductivity of KOH solution. (d) Influence of KOH solution concentration on electrical resistance and exergy efficiency.

5.2.3. Influence of bubble coverage

The bubbles generate by the reaction will firstly adhere to the surface of the electrode, which will reduce the effective area of the electrode and cause the increase

of the actual current density, then lead to the increase of activation over-potential [30]. The increase of bubbles content in the solution will increase the ion migration resistance and lead to the increase of ohmic over-potential. In the reaction process, bubble coverage is used to indicate the proportion of the area covered by the bubbles to the total surface area of the electrode. Fig. 7 show the influence of bubble coverage on ohmic over-potential, activated over-potential and exergy efficiency. According to Fig. 7(a), the proportions of both ohmic and activated over-potential in total voltage will increase with bubble coverage, and the former is more sensitive than the latter one to bubble coverage rate. The activation over-potential increases 0.05 V from 0.56 V to 0.61 V, at same time the ohmic over-potential increases by 0.07 V from 0.27 V to 0.34 V when the bubble coverage rate increasing from 0 to 50%. Fig. 7(b) shows the influence of the bubble coverage on the bubble resistance and exergy efficiency. Bubble resistance increase from 0 to 2.3×10^{-4} Ω when the bubble coverage increasing from 0 to 50%, which leads the exergy efficiency decreases 3.3% from 60.4% to 57.1%. The bubble coverage has a significant impact on exergy efficiency from the analysis results. However, from the perspective of the influence of current density on bubble coverage as shown in Fig. 7(c), the bubble coverage greatly increases from 0 to 22.5% when the current density increases from 0 to 5000 $\mathrm{A/m^2}$, and the exergy efficiency slightly decreases 1.2% from 60.4% to 59.2%. The bubble coverage only increases 5.2% from 22.5% to 27.7% when the current density increases from 5000 $\mathrm{A/m^2}$ to 10000 $\mathrm{A/m^2}$, at the same time, the exergy efficiency decreases only 0.3% from 59.2% to 58.9%. This result shows that bubble coverage caused by reaction has just a little influence on

over-potential and exergy efficiency in actual reaction, even though bubble coverage is quite sensitive to current density. Kraglund et al. [41] tested the current resistance of electrolyzer under different current densities based on EIS experiments, and found that the overall resistance increases slightly when the current density increasing from 800 A/m^2 to 12000 A/m^2. Because the change of current density has the greatest impact on bubble resistance when electrolyte flow rate and other conditions remain unchanged, so the change in bubble coverage caused by current density is not the main factor affecting the loss of over-potential and exergy efficiency.

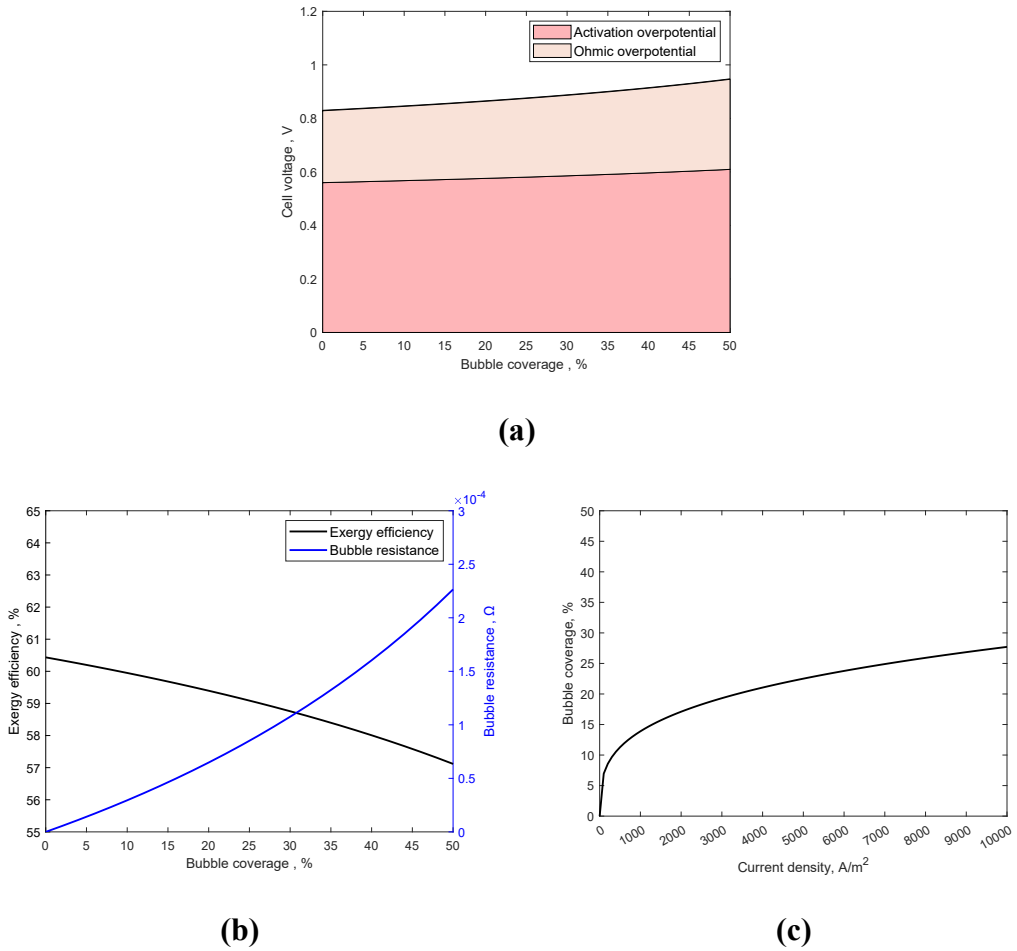

Fig. 7. Influence of bubble coverage. (a) Influence of bubble coverage on ohmic and activation over-potential. (b) Influence of bubble coverage on

electrical resistance and exergy efficiency. (c) Influence of current density on bubble coverage.

In this section, the influence of each characteristic parameter on exergy efficiency and the exergy loss due to different resistances are compared in detail. Diaphragm resistance takes up the largest proportion of the total ohmic resistance, followed by electrolyte resistance and then bubble resistance, and electrode resistance has the smallest proportion. The diaphragm porosity has very significant effect on exergy efficiency by affecting the diaphragm resistance. And the electrode gap has also an obvious but lower effect than diaphragm porosity on exergy efficiency by affecting electrolyte resistance, but its effect can be minimized when applying a zero-gap electrolyzer structure. The proportion of bubble resistance in total ohmic resistance is relatively small and the bubble coverage has just a small effect on exergy efficiency, but it has an effect on both activation and ohmic over-potential, so it is still very important to investigate methods to reduce bubble coverage, such as flow channel design and the choice of optimum flow rate. The proportion of electrode resistance in total ohmic resistance is approximately negligible, therefore, further improving of electrode conductivity is meaningless.

5.3. Analysis of the influence of operating conditions on exergy efficiency

The temperature, pressure and other operating conditions of the electrolyzer can also influence on the cell voltage and exergy efficiency. This section will conduct a quantitative analysis of the influence of temperature and pressure on exergy efficiency.

Increasing pressure will increase reversible voltage, while decrease bubble coverage thus reduce bubble resistance. Fig. 8(a) shows the influence of pressure on cell voltage and exergy efficiency at 358 K with 5000 A/m^2. It can be seen that reversible cell voltage slightly increases 0.05V from 1.18 V to 1.23 V as pressure increasing from 1×10^6 Pa to 5×10^6 Pa. Synchronously, activation over-potential decreases 0.03 V from 0.59 V to 0.56 V and ohmic over-potential decreases 0.02 V from 0.3 V to 0.28 V. As a result, both cell voltage and exergy efficiency are firstly a little improved and then slightly decreased, and achieve its maximum at the pressure of 3.5×10^6 Pa. It is mainly because, as the pressure increasing, over-potential reducing rate is greater but then smaller than reversible voltage growing rate. As the pressure increasing from 1×10^6 Pa to 3.5×10^6 Pa, the cell voltage only decreases 0,02 V from 2.08 V to 2.06 V, as a result, exergy efficiency slightly increases 0.5% from 58.9% to 59.4%. While, as the pressure further increasing from 3.5×10^6 Pa to 5×10^6 Pa, the reducing rate of over-potential is only slightly lower than increasing rate of reversible voltage, resulting the electrolytic voltage only increased slightly on the basis of 2.06 V, with an increase of less than 0.01 V, and the increase of exergy efficiency is less than 0.1%. To sum up, there is the best pressure to achieve the best exergy efficiency of the electrolyzer, even though the influence of pressure on cell voltage and exergy efficiency is not significant. It should be noted that increasing the reaction pressure can reduce the cost and energy consumption of hydrogen compression, but unfortunately, will synchronously reduce hydrogen purity and squeeze AWE operation range.

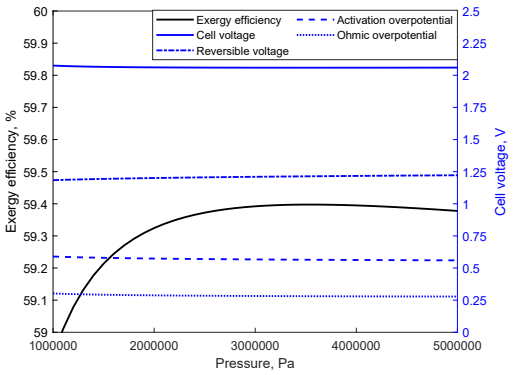

(a)

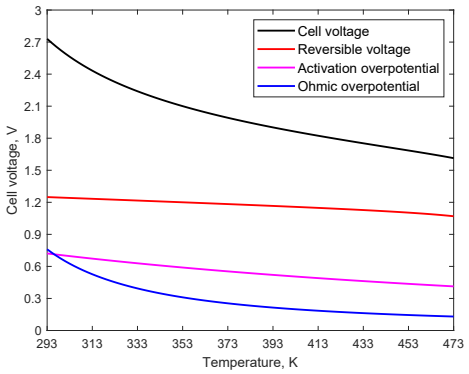

(b)

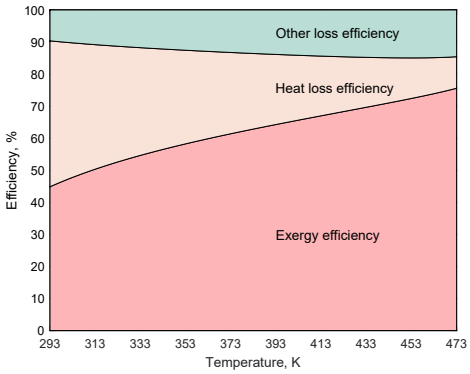

(c)

Fig. 8. Effect of pressure and temperature. (a) Influence of pressure on voltage and exergy efficiency (b) Influence of temperature on cell voltage. (c) Influence of temperature on exergy efficiency.

Temperature presents an obviously influence on exergy efficiency and voltage loss. In addition to its direct influence on reversible voltage and activation over-potential, temperature can indirectly affect the electrolytic voltage of each part by affecting water activity, water vapor partial pressure, bubble coverage and ionic conductivity. The influence of temperature on the cell voltage and exergy efficiency at 1.6×10^6 Pa pressure with 5000 $\mathrm{A/m^2}$ is shown in Fig. 8(b) and Fig. 8(c). Temperature, compared with pressure, its influence on the cell voltage and exergy efficiency is more significant.

As shown in Fig. 8(b), increasing temperature is beneficial to decrease reversible electrolytic voltage, ohmic over-potential and activation over-potential, which has a more significant effect on ohmic over-potential, followed by activation over-potential, and has the least effect on reversible electrolytic voltage. As the temperature increasing from 293 K to 373 K, the cell voltage decreases 0.74 V from 2.73 V to 1.99 V, the ohmic over-potential significantly decreases 0.51 V from 0.76 V to 0.25 V, the activation over-potential decreases 0.17 V from 0.72 V to 0.55 V, the reversible voltage slightly decreases 0.07 V from 1.25 V to 1.18 V. As the temperature further rising from 373 K to 473K, the reduction range of electrolytic voltage gradually decreased from 1.99 V to 1.61 V, decreased by 0.38 V, the decrease of ohmic over-potential gradually becomes gentle which decreased by 0.12 V from 0.25 V to 0.13 V, the reversible electrolytic voltage and activation over-potential remained approximately linear, in which the activation over-potential slightly increased by 0.14 V from 0.55 V to 0.41 V, the reversible electrolytic voltage decreased from 1.18 V to 1.07 V, decreasing by 0.11 V.

The influence of temperature on exergy efficiency is shown in Fig. 8(c). Increasing temperature promotes over-potential reducing, then causes the thermal loss efficiency decreasing and exergy efficiency increasing with a decelerated rate. Exergy efficiency increases almost linearly in the range of 293 K to 473 K. As the temperature increasing from 293 K to 373 K, exergy efficiency significantly improves 16.5% from 44.9% to 61.4%, at the same time, heat loss efficiency greatly drops 20.2% from 45.5% to 25.3%. The exergy efficiency increases 14.2% from 61.4% to 75.6%, and heat loss efficiency

decreases 15.5% from 25.3% to 9.8% when the temperature further increasing from 373 K to 473 K. In conclusion, temperature has a significant impact on electrolytic voltage and exergy efficiency, but with the further increase of temperature, the improvement effect on exergy efficiency will gradually weaken. From the analysis results, increasing temperature is beneficial to improve the electrolysis efficiency. But from the perspective of the energy use of electrolytic system, too high reaction temperature may cause the power consumption of the attachment system increases, which is not conducive to improve the energy efficiency of the whole system [17]. At the same time, too high temperature can cause the electrolyte boiling which is easy to cause safety problems, it will also pose greater challenges to the heat resistant performance of diaphragm and gasket.

6. Conclusions

This paper establishes a comprehensive electrochemical model of AWE electrolyzer which is calibrated with experimental data to study the changing trend of cell voltage during electrolysis. According to the comprehensive electrochemical-thermodynamic model, the change of exergy efficiency with current density and the loss of exergy efficiency caused by various characteristic parameters and operating conditions are predicted. The conclusions are as follows:

- Activation over-potential, compared with ohmic over-potential, presents more significant influence on the cell voltage and exergy loss with the increase of current density. Exergy loss caused by ohmic over-potential changes most

obviously. Diaphragm resistance accounts for the largest proportion of total ohmic resistance exergy loss, followed by electrolyte and bubble, and exergy loss caused by electrode can be almost ignored.

- Exergy efficiency just slightly increases 0.4% from 58.7% to 59.1% when the electrode conductivity increases from 1000 S/m to 6000 S/m. because electrode resistance is small at first, therefore, there is little room for improving exergy efficiency by improving electrode conductivity.
- The electrode gap changes from 0 mm to 10 mm causes exergy efficiency drops 11.3% from 62.4% to 51.1%, which has a significant effect on exergy efficiency. The electrode gap should be reduced as much as possible under the condition that the efflux of bubbles on the electrode surface is not affected.
- Increasing diaphragm porosity and decreasing tortuosity are beneficial to reduce the resistance of ions across the diaphragm. The exergy efficiency significantly increases 18.4% from 40.8% to 59.2% when the porosity increases from 0.1 to 0.6. The tortuosity changes from 1 to 6 causes the exergy efficiency decreases 5.9% from 63.8% to 57.9%. Increasing porosity, compared with decreasing tortuosity, presents a more significant effect on reducing diaphragm resistance and improving exergy efficiency.
- Electrolyte conductivity has an impact on the resistance of electrolyte, diaphragm and bubbles. Existing the best electrolyte concentration at different temperature to achieve the highest conductivity. The exergy efficiency rapidly increases from 0% to 52.1% when KOH molar concentration changing from

0 mol/L to 2 mol/L; it slowly increases 7.2% from 52.1% to 59.3% as the concentration increasing from 2 mol/L to 7 mol/L; while, it will remain constant or even slightly decrease when the concentration further increasing from 7 mol/L.

- Increasing the bubble coverage will lead to an increase in over-potential and a decrease in exergy efficiency. The exergy efficiency decreases 3.3% from 60.4% to 57.1% when the bubble coverage increases from 0 to 50%. However, the change of bubble coverage caused by current density in actual reaction has no obvious influence on over-potential and exergy efficiency. The bubble coverage is about 27.7% when the current density reaches to 10000 A/m^2. At this time, the exergy efficiency is 58.9%, which is just slightly decreasing 0.3% than that at 5000 A/m^2.
- The temperature and pressure also affect the cell voltage and exergy efficiency. From the perspective of pressure, there exists the best pressure to make the cell voltage and exergy efficiency reach the best value. Exergy efficiency reaches the best value of 59.4% when the pressure is 3.5×10^6 Pa. Increasing reaction temperature can help to reduce cell voltage and improve exergy efficiency. The efficiency increases almost linearly when the temperature increases from 293 K to 473 K, but its growth between 373 K−473 K is slightly lower than that between 293 K−373 K. The exergy efficiency significantly improves 16.5% from 44.9% to 61.4% when the temperature increasing from 293 K to 373 K. And it increases 14.2% from 61.4% to 75.6%,

when the temperature further increasing from 373 K to 473 K.

Acknowledgement

The authors would like to thank Yayang Jiang and Jinwei Sun from State Key Laboratory of Automotive Safety and Energy in Tsinghua University for their help in the experiments and simulations. This work is sponsored by the State Key Laboratory of Automotive Safety and Energy under Project (No. KFY2219), China Postdoctoral Science Foundation (No. 2021M691733), National Natural Science Foundation of China (51906225), Key R&D and Promotion Project in Henan Province (192102210225), and Shell-Tsinghua Joint Project (Contract No. PT70943) from Shell.

References

[1] Fatouh M, Shedid M H, Elshokary S. Effect of operating and geometric parameters on hydrogen production from an alkali electrolyzer[J]. International Association for Hydrogen Energy. 2013.

[2] Yang F, Wang T, Deng X, et al. Review on hydrogen safety issues: Incident statistics, hydrogen diffusion, and detonation process[J]. International journal of hydrogen energy. 2021, 46(61): 31467-31488.

[3] Yang M, Hu S, Yang F, et al. On-board Liquid Hydrogen Cold Energy Utilization System for A Heavy-duty Fuel Cell Hybrid Truck[J]. World Electric Vehicle Journal. 2021.

[4] Song Hu S D A R. Comparison of Physics-Based, Semi-empirical and Neural Network-based Models for Model-based Combustion Control in a 3.0 L Diesel Engine[J]. Energies. 2019.

[5] Greene D L, Ogden J M, Lin Z. Challenges in the designing, planning and deployment of hydrogen refueling infrastructure for fuel cell electric vehicles[J]. eTransportation. 2020, 6: 100086.

[6] Qi Y, Espinoza-Andaluz M, Thern M, et al. Polymer electrolyte fuel cell system level modelling and simulation of transient behavior[J]. eTransportation. 2019, 2: 100030.

[7] Olivier P, Bourasseau C, Bouamama P B. Low-temperature electrolysis system modelling: A review[J]. Renewable and Sustainable Energy Reviews. 2017, 78: 280-300.

[8] Zakeri B, Syri S. Electrical energy storage systems: A comparative life cycle cost analysis[J]. Renewable & sustainable energy reviews. 2015, 42: 569-596.

[9] Suleman F, Dincer I, Agelin-Chaab M. Comparative impact assessment study of various hydrogen production methods in terms of emissions[J]. International journal of hydrogen energy. 2016, 41(19): 8364-8375.

[10] Lonis F, Tola V, Cau G. Assessment of integrated energy systems for the production and use of

renewable methanol by water electrolysis and CO2 hydrogenation[J]. Fuel (Guildford). 2021, 285: 119160.

[11] David M, Ocampo-Martínez C, Sánchez-Peña R. Advances in alkaline water electrolyzers: A review[J]. Journal of Energy Storage. 2019, 23: 392-403.

[12] Ulleberg. Modeling of advanced alkaline electrolyzers: a system simulation approach[J]. International Journal of Hydrogen Energy. 2003, 28(1): 21-33.

[13] Artuso P, Gammon R, Orecchini F, et al. Alkaline electrolysers: Model and real data analysis[J]. International Journal of Hydrogen Energy. 2011, 36(13): 7956-7962.

[14] Khalilnejad A, Riahy G H. A hybrid wind-PV system performance investigation for the purpose of maximum hydrogen production and storage using advanced alkaline electrolyzer[J]. Energy conversion and management. 2014, 80: 398-406.

[15] Varela C, Mostafa M, Zondervan E. Modeling alkaline water electrolysis for power-to-x applications: A scheduling approach[J]. International journal of hydrogen energy. 2021, 46(14): 9303-9313.

[16] Henao C, Agbossou K, Hammoudi M, et al. Simulation tool based on a physics model and an electrical analogy for an alkaline electrolyser[J]. Journal of Power Sources. 2014, 250: 58-67.

[17] Jang D, Cho H, Kang S. Numerical modeling and analysis of the effect of pressure on the performance of an alkaline water electrolysis system[J]. Applied energy. 2021, 287: 116554.

[18] Jang D, Choi W, Cho H, et al. Numerical modeling and analysis of the temperature effect on the performance of an alkaline water electrolysis system[J]. Journal of Power Sources. 2021, 506: 230106.

[19] Sandeep K C, Kamath S, Mistry K, et al. Experimental studies and modeling of advanced alkaline water electrolyser with porous nickel electrodes for hydrogen production[J]. International Journal of

Hydrogen Energy. 2017, 42(17): 12094-12103.

[20] Zeng K, Zhang D. Recent progress in alkaline water electrolysis for hydrogen production and applications[J]. Progress in Energy and Combustion Science. 2010, 36(3): 307-326.

[21] Bakker M M, Vermaas D A. Gas bubble removal in alkaline water electrolysis with utilization of pressure swings[J]. Electrochimica Acta. 2019, 319: 148-157.

[22] Robert P, Dunnill C W. Zero gap alkaline electrolysis cell design for renewable energy storage as hydrogen gas[J]. RSC advances. 2016, 6(12): 1643-1651.

[23] Haverkort J W, Rajaei H. Voltage losses in zero-gap alkaline water electrolysis[J]. Journal of Power Sources. 2021, 497: 229864.

[24] Li Y, Chen Y. The effect of magnetic field on the dynamics of gas bubbles in water electrolysis[J]. Scientific Reports. 2021, 11(1).

[25] Wang M, Wang Z, Guo Z. Water electrolysis enhanced by super gravity field for hydrogen production[J]. International Journal of Hydrogen Energy. 2010, 35(8): 3198-3205.

[26] Li S, Wang C, Chen C. Water electrolysis in the presence of an ultrasonic field[J]. Electrochimica Acta. 2009, 54(15): 3877-3883.

[27] Zouhri K, Lee S. Evaluation and optimization of the alkaline water electrolysis ohmic polarization: Exergy study[J]. International journal of hydrogen energy. 2016, 41(18): 7253-7263.

[28] Ni M, Leung M K H, Leung D Y C. Energy and exergy analysis of hydrogen production by a proton exchange membrane (PEM) electrolyzer plant[J]. Energy conversion and management. 2008, 49(10): 2748-2756.

[29] Ni M, Leung M K H, Leung D Y C. Energy and exergy analysis of hydrogen production by solid oxide steam electrolyzer plant[J]. International journal of hydrogen energy. 2007, 32(18): 4648-4660.

[30] Hammoudi M, Henao C, Agbossou K, et al. New multi-physics approach for modelling and design of alkaline electrolyzers[J]. International journal of hydrogen energy. 2012, 37(19): 13895-13913.

[31] J B. Water vapour partial pressures and water activities in potassium and sodium hydroxide solutions over wide concentration and temperature ranges[J]. Hydrogen Energy. 1985.

[32] Li Y, Pei P, Wu Z, et al. Approaches to avoid flooding in association with pressure drop in proton exchange membrane fuel cells[J]. Applied energy. 2018, 224: 42-51.

[33] Kienzlen V, Haaf D, Schnurnberger W. Location of hydrogen gas evolution on perforated plate electrodes in zero gap cells[J]. International Journal of Hydrogen Energy. 1994.

[34] Gilliam R, Graydon J, Kirk D, et al. A review of specific conductivities of potassium hydroxide solutions for various concentrations and temperatures[J]. International Journal of Hydrogen Energy. 2007, 32(3): 359-364.

[35] Rodríguez, Palmas, Sánchez-Molina, et al. Simple and Precise Approach for Determination of Ohmic Contribution of Diaphragms in Alkaline Water Electrolysis[J]. Membranes (Basel). 2019, 9(10): 129.

[36] Barco-Burgos J, Eicker U, Saldaña-Robles N, et al. Thermal characterization of an alkaline electrolysis cell for hydrogen production at atmospheric pressure[J]. Fuel. 2020, 276: 117910.

[37] Chan S H, Low C F, Ding O L. Energy and exergy analysis of simple solid-oxide fuel-cell power systems[J]. Journal of power sources. 2002, 103(2): 188-200.

[38] Herdem M S, Farhad S, Dincer I, et al. Thermodynamic modeling and assessment of a combined coal gasification and alkaline water electrolysis system for hydrogen production[J]. International journal of hydrogen energy. 2014, 39(7): 3061-3071.

[39] Zhang M, Gao Y, Zhang Y, et al. Preparation and properties of polyphenylene sulfide/oxidized-

polyphenylene sulfide composite membranes[J]. Reactive & functional polymers. 2021, 160: 104842.

[40] Lee J, Alam A, Park C, et al. Modeling of gas evolution processes in porous electrodes of zero-gap alkaline water electrolysis cells[J]. Fuel (Guildford). 2022, 315.

[41] Kraglund M R. Alkaline membrane water electrolysis with non-noble catalysts[J]. 2017.